



ELSEVIER

# Reactions of thioarsines with metal carbonyls: synthesis and structural characterisation of $[\text{Fe}_2(\text{CO})_6(\mu\text{-AsMe}_2)(\mu\text{-SPh})]$ , $[\text{Fe}_2\text{Cp}_2(\text{CO})_2(\mu\text{-AsPh}_2)(\mu\text{-SPh})]$ , $[\text{Mn}_2(\text{CO})_8(\mu\text{-AsPh}_2)(\mu\text{-SPh})]$ and $[\text{Co}_3(\mu_3\text{-S})(\mu\text{-AsPh}_2)(\text{CO})_6\text{AsPh}_3]$

Gráinne Conole<sup>a</sup>, John E. Davies<sup>b</sup>, Jason D. King<sup>b</sup>, Martin J. Mays<sup>b,\*</sup>,  
Mary McPartlin<sup>a</sup>, Harold R. Powell<sup>b</sup>, Paul R. Raithby<sup>b</sup>

<sup>a</sup> School of Applied Chemistry, University of North London, Holloway Rd., London N7 8DB, UK

<sup>b</sup> Department of Chemistry, Lensfield Rd., Cambridge CB2 1EW, UK

Received 24 February 1999; received in revised form 8 April 1999

## Abstract

The thioarsine,  $\text{AsMe}_2(\text{SPh})$ , reacts thermally with  $[\text{Fe}(\text{CO})_5]$  to give the new bimetallic butterfly complex,  $[\text{Fe}_2(\text{CO})_6(\mu\text{-AsMe}_2)(\mu\text{-SPh})]$  (**1**). Similarly, thermolysis of the thioarsine  $\text{AsPh}_2(\text{SPh})$  with  $[\text{Fe}_2\text{Cp}_2(\text{CO})_4]$  and  $[\text{Mn}_2(\text{CO})_{10}]$  affords, respectively  $[\text{Fe}_2\text{Cp}_2(\text{CO})_2(\mu\text{-AsPh}_2)(\mu\text{-SPh})]$  (**2**) and  $[\text{Mn}_2(\text{CO})_8(\mu\text{-AsPh}_2)(\mu\text{-SPh})]$  (**3**). At room temperature,  $\text{AsPh}_2(\text{SPh})$  reacts rapidly with  $[\text{Co}_2(\text{CO})_8]$  to yield the trimetallic product,  $[\text{Co}_3(\mu_3\text{-S})(\mu\text{-AsPh}_2)(\text{CO})_6\text{AsPh}_3]$  (**4**). The crystal structures of these four products have been determined by X-ray crystallography. Arsenic–sulfur bond cleavage is a feature of all these reactions; concomitant arsenic–carbon bond formation is observed in the production of complex **4**. © 1999 Elsevier Science S.A. All rights reserved.

**Keywords:** Bimetallic complexes; Cobalt; Crystal structure; Iron; Manganese; Thioarsines

## 1. Introduction

A substantial amount of work has been carried out on the scission of P–S bonds within the coordination sphere of metal carbonyl complexes. Thus, thermolytic reaction of the thiophosphine,  $\text{PPh}_2(\text{SPh})$  with  $[\text{Fe}(\text{CO})_5]$  affords the di-iron complex,  $[\text{Fe}_2(\text{CO})_6(\mu\text{-PPh}_2)(\mu\text{-SPh})]$  [1,2] and, more recently, it has been shown that  $[\text{Mn}_2(\text{CO})_{10}]$  reacts with the same ligand at 150°C to yield a similar bimetallic product,  $[\text{Mn}_2(\mu\text{-PPh}_2)(\mu\text{-SPh})(\text{CO})_8]$  [3].

The reaction of this thiophosphine with  $[\text{Co}_2(\text{CO})_8]$  does not lead to mixed-bridged dicobalt species but instead a complex with a  $\text{Co}_3\text{S}$  tetrahedrane core is formed in which a  $\text{PPh}_2$  group bridges one of the

Co–Co edges [3]. Tetrahedrane products are also produced in the reactions of the related thiophosphine,  $\text{PPh}_2(\text{S}'\text{Bu})$ , with  $[\text{Fe}(\text{CO})_5]$  or with a mixture of  $[\text{Fe}(\text{CO})_5]$  and  $[\text{Co}_2(\text{CO})_8]$ ; heterotrimetallic complexes are generated in the latter reaction [4].

Rupture of the P–S bond is also a feature of the reactions of a number of thiophosphines,  $\text{PPh}_2(\text{SR})$  [ $\text{R} = \text{Ph}$ ,  $t\text{Bu}$ ,  $n\text{Bu}$ ], with alkyne-bridged dicobalt hexacarbonyl complexes, and these reactions lead to a variety of metallacyclic products containing sulfur or phosphorus within the ring [4,5].

Although the metal-mediated breaking of As–S bonds in inorganic molecules such as  $\text{As}_4\text{S}_4$  has received considerable attention [6], the cleavage of As–S bonds in thioarsines remains relatively unexplored. In this paper we report, for comparison with the work on P–S bond cleavage in thiophosphines, the results of our investigations into the reactions of the thioarsines  $\text{AsPh}_2(\text{SPh})$  and  $\text{AsMe}_2(\text{SPh})$  with a variety of metal carbonyl complexes.

\* Corresponding author. Fax: +44-1223-336362.

E-mail address: mjm14@cam.ac.uk (M.J. Mays)

## 2. Results and discussion

### 2.1. Reaction of $AsMe_2(SPh)$ with $[Fe(CO)_5]$

Reaction of  $AsMe_2SPh$  with  $[Fe(CO)_5]$  in refluxing toluene gave orange crystalline  $[Fe_2(CO)_6(\mu-AsMe_2)_2]$  (28%) and yellow crystalline  $[Fe_2(CO)_6(\mu-AsMe_2)(\mu-SPh)]$  (**1**) (36%). Complex **1** has been characterised by IR,  $^1H$ - and  $^{13}C$ -NMR spectroscopy, mass spectrometry and microanalysis. In addition, the complex has been the subject of a single-crystal X-ray diffraction study.  $[Fe_2(CO)_6(\mu-AsMe_2)_2]$  was identified by reference to published data for this known compound [7].

The molecular structure of **1** is shown in Fig. 1. Selected bond lengths and angles are presented in

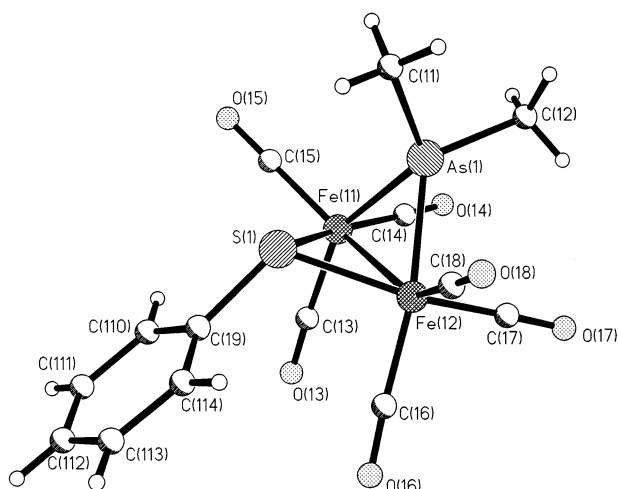


Fig. 1. Molecular structure of  $[Fe_2(CO)_6(\mu-AsMe_2)(\mu-SPh)]$  (**1**) including atom numbering scheme.

Table 1a

Selected bond lengths (Å) and angles (°) for  $Fe_2(CO)_6(\mu-AsMe_2)(\mu-SPh)$  (**1**) molecule 1

Fe(11)–Fe(12)	2.599(2)	As(1)–Fe(11)–Fe(12)	56.26(4)
As(1)–Fe(11)	2.3065(14)	As(1)–Fe(12)–Fe(11)	55.51(4)
As(1)–Fe(12)	2.327(2)	S(1)–Fe(11)–Fe(12)	55.10(7)
Fe(11)–S(1)	2.266(2)	S(1)–Fe(12)–Fe(11)	54.97(6)
Fe(12)–S(1)	2.269(2)	S(1)–Fe(11)–As(1)	77.50(7)
As(1)–C(11)	1.932(10)	S(1)–Fe(12)–As(1)	77.01(7)
As(1)–C(12)	1.935(10)	Fe(11)–S(1)–Fe(12)	69.93(7)
S(1)–C(19)	1.784(9)	Fe(11)–As(1)–Fe(12)	68.23(5)
Fe(11)–C(13)	1.785(10)	C(19)–S(1)–Fe(11)	115.0(3)
Fe(11)–C(14)	1.757(10)	C(19)–S(1)–Fe(12)	116.1(3)
Fe(11)–C(15)	1.785(11)	C(11)–As(1)–C(12)	102.7(6)
Fe(12)–C(16)	1.793(10)	C(11)–As(1)–Fe(11)	122.7(4)
Fe(12)–C(17)	1.772(10)	C(12)–As(1)–Fe(11)	122.0(4)
Fe(12)–C(18)	1.780(10)	C(11)–As(1)–Fe(12)	117.9(4)
O(13)–C(13)	1.132(11)	C(12)–As(1)–Fe(12)	121.8(4)
O(14)–C(14)	1.134(12)	C(13)–Fe(11)–Fe(12)	94.6(3)
O(15)–C(15)	1.142(11)	C(14)–Fe(11)–Fe(12)	108.6(4)
O(16)–C(16)	1.129(11)	C(15)–Fe(11)–Fe(12)	147.4(3)
O(17)–C(17)	1.133(11)	C(16)–Fe(12)–Fe(11)	105.1(3)
O(18)–C(18)	1.143(11)	C(17)–Fe(12)–Fe(11)	99.4(3)

Table 1b

Selected bond lengths (Å) and angles (°) for  $Fe_2(CO)_6(\mu-AsMe_2)(\mu-SPh)$  (**1**) molecule 2

Fe(21)–Fe(22)	2.613(2)	As(2)–Fe(21)–Fe(22)	55.94(4)
As(2)–Fe(21)	2.3127(14)	As(2)–Fe(22)–Fe(21)	55.49(4)
As(2)–Fe(22)	2.3253(14)	S(2)–Fe(21)–Fe(22)	54.89(7)
Fe(21)–S(2)	2.259(2)	S(2)–Fe(22)–As(2)	76.56(7)
Fe(22)–S(2)	2.267(3)	S(2)–Fe(21)–As(2)	76.97(7)
As(2)–C(21)	1.935(10)	S(2)–Fe(22)–Fe(21)	54.59(7)
As(2)–C(22)	1.936(10)	Fe(21)–S(2)–Fe(22)	70.52(7)
S(2)–C(29)	1.773(9)	Fe(21)–As(2)–Fe(22)	68.57(5)
Fe(21)–C(23)	1.799(9)	C(29)–S(2)–Fe(21)	115.4(3)
Fe(21)–C(24)	1.765(9)	C(29)–S(2)–Fe(22)	116.5(3)
Fe(21)–C(25)	1.791(10)	C(21)–As(2)–C(22)	102.8(5)
Fe(22)–C(26)	1.793(10)	C(21)–As(2)–Fe(21)	119.8(4)
Fe(22)–C(27)	1.772(11)	C(22)–As(2)–Fe(21)	122.5(3)
Fe(22)–C(28)	1.784(11)	C(21)–As(2)–Fe(22)	120.6(3)
O(23)–C(23)	1.121(10)	C(22)–As(2)–Fe(22)	121.2(3)
O(24)–C(24)	1.134(10)	C(23)–Fe(21)–Fe(22)	97.4(3)
O(25)–C(25)	1.136(10)	C(24)–Fe(21)–Fe(22)	106.2(3)
O(26)–C(26)	1.137(11)	C(25)–Fe(21)–Fe(22)	149.2(3)
O(27)–C(27)	1.149(12)	C(26)–Fe(22)–Fe(21)	102.4(3)
O(28)–C(28)	1.135(12)	C(27)–Fe(22)–Fe(21)	102.4(3)
		C(28)–Fe(22)–Fe(21)	147.0(4)

Table 1c

Selected bond lengths (Å) and angles (°) for  $Fe_2(CO)_6(\mu-AsMe_2)(\mu-SPh)$  (**1**) molecule 3

Fe(31)–Fe(32)	2.577(2)	As(3)–Fe(31)–Fe(32)	56.29(4)
As(3)–Fe(31)	2.330(2)	As(3)–Fe(32)–Fe(31)	56.48(4)
As(3)–Fe(32)	2.325(2)	S(3)–Fe(31)–Fe(32)	55.23(7)
Fe(31)–S(3)	2.257(2)	S(3)–Fe(32)–As(3)	55.17(6)
Fe(32)–S(3)	2.258(2)	S(3)–Fe(31)–As(3)	77.06(7)
As(3)–C(31)	1.938(10)	S(3)–Fe(32)–As(3)	77.14(7)
As(3)–C(32)	1.935(10)	Fe(31)–S(3)–Fe(32)	69.60(7)
S(3)–C(39)	1.780(8)	Fe(32)–As(3)–Fe(31)	67.23(5)
Fe(31)–C(33)	1.790(10)	C(39)–S(3)–Fe(31)	116.2(3)
Fe(31)–C(34)	1.758(11)	C(39)–S(3)–Fe(32)	115.7(3)
Fe(31)–C(35)	1.782(10)	C(32)–As(3)–C(31)	102.5(5)
Fe(32)–C(36)	1.807(10)	C(31)–As(3)–Fe(31)	121.3(4)
Fe(32)–C(37)	1.766(12)	C(32)–As(3)–Fe(31)	122.8(4)
Fe(32)–C(38)	1.781(12)	C(31)–As(3)–Fe(32)	118.9(4)
O(33)–C(33)	1.139(11)	C(32)–As(3)–Fe(32)	122.7(3)
O(34)–C(34)	1.152(12)	C(33)–Fe(31)–Fe(32)	97.9(3)
O(35)–C(35)	1.146(11)	C(34)–Fe(31)–Fe(32)	102.7(4)
O(36)–C(36)	1.130(11)	C(35)–Fe(31)–Fe(32)	149.6(3)
O(37)–C(37)	1.145(13)	C(36)–Fe(32)–Fe(31)	99.8(3)
O(38)–C(38)	1.139(13)	C(37)–Fe(32)–Fe(31)	100.4(4)
		C(38)–Fe(32)–Fe(31)	147.4(4)

Tables 1a–c. The complex crystallizes with three molecules in the asymmetric unit. No major differences are noted in the overall geometries of these three molecules. Bond lengths and angles for molecule **1** are used in the following discussion.

The localized environment about each iron atom, neglecting any metal–metal bonding, may be pictured as a distorted tetragonal pyramid with a carbonyl ligand in the apical position and the square base composed of the remaining two CO ligands and the

bridging arsenic and sulfur atoms. The iron atoms are situated a mean distance of 0.37 Å out of this basal plane towards the apical carbonyl ligand.

The 18-electron rule requires the presence of a metal–metal bond and inclusion of this interaction produces a distorted octahedral arrangement about each metal atom. Fig. 1 thus displays the molecule as a ‘butterfly’ structure with the AsMe<sub>2</sub> and SPh groups at the wing-tips with an angle of 98.5° between the Fe–Fe–As and Fe–Fe–S planes.

The Fe–Fe distance of 2.599(2) Å in **1** is shorter than in [Fe<sub>2</sub>(CO)<sub>6</sub>(μ-AsMe<sub>2</sub>)<sub>2</sub>] [8] (2.733(4) and 2.726(4) Å) but longer than that in [Fe<sub>2</sub>(CO)<sub>6</sub>(μ-SEt)<sub>2</sub>] [9] (2.507(5) Å) and very close to those found in the complexes [Fe<sub>2</sub>(CO)<sub>6</sub>(μ-AsPh<sub>2</sub>)(μ-S<sup>i</sup>Pr)] [10] (2.626 Å) and [Fe<sub>2</sub>(CO)<sub>6</sub>(μ-S<sup>i</sup>Bu)(AsMe)<sub>2</sub>] [11] (2.586(1) and 2.596(1) Å), which are the only other reported species containing an Fe<sub>2</sub>AsS butterfly core. The Fe–As bond lengths (2.3065(14) and 2.327(2) Å) are comparable to those measured in a wide range of complexes containing an arsenido-bridged Fe–Fe bond (2.31–2.40 Å) [8]. The Fe–S bond lengths of 2.266(2) and 2.269(2) Å are almost exactly that found in the only other complex of this type with one arsenido and one thiolato group, [Fe<sub>2</sub>(CO)<sub>6</sub>(μ-AsPh<sub>2</sub>)(μ-S<sup>i</sup>Pr)] [10] (2.264 Å).

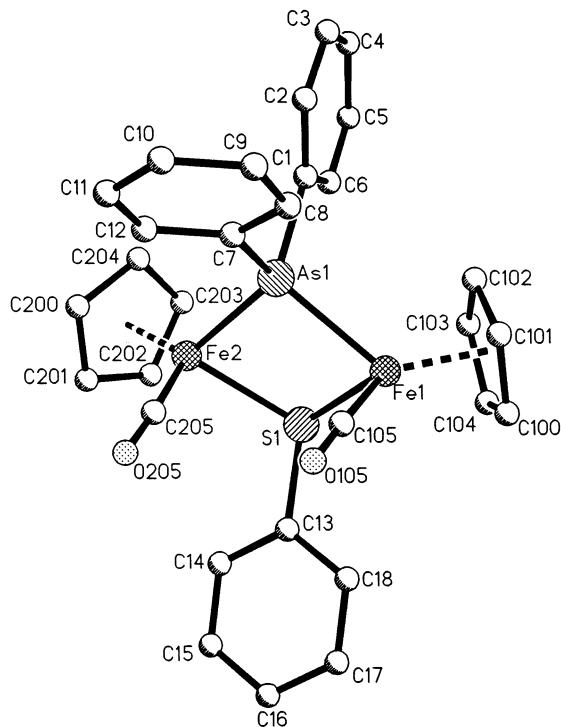


Fig. 2. Molecular structure of [Fe<sub>2</sub>Cp<sub>2</sub>(CO)<sub>2</sub>(μ-AsPh<sub>2</sub>)(μ-SPh)] (**2**) including atom numbering scheme. Hydrogen atoms have been omitted for clarity.

Table 2

Selected bond lengths (Å) and angles (°) for Fe<sub>2</sub>Cp<sub>2</sub>(CO)<sub>4</sub>(μ-AsPh<sub>2</sub>)(μ-SPh) (**2**)

Fe(1)–As(1)	2.3504(7)	S(1)–Fe(1)–As(1)	78.13(3)
Fe(2)–As(1)	2.3460(7)	S(1)–Fe(2)–As(1)	78.32(3)
Fe(1)–S(1)	2.2965(11)	Fe(2)–As(1)–Fe(1)	98.72(2)
Fe(2)–S(1)	2.2920(10)	Fe(2)–S(1)–Fe(1)	101.91(4)
Fe(1)–C <sub>carbonyl</sub>	1.748(4)	C(105)–Fe(1)–S(1)	96.05(13)
Fe(2)–C <sub>carbonyl</sub>	1.754(4)	C(105)–Fe(1)–As(1)	89.51(14)
C(105)–O(105)	1.154(5)	C(205)–Fe(2)–S(1)	94.25(14)
C(205)–O(205)	1.149(5)	C(205)–Fe(2)–As(1)	91.53(14)
Fe(1)–C <sub>Cp</sub>	2.080(4)–2.110(4)	C(7)–As(1)–Fe(1)	116.59(12)
As(1)–C(1)	1.968(4)	C(7)–As(1)–Fe(2)	115.02(12)
As(1)–C(7)	1.959(4)	C(1)–As(1)–Fe(1)	112.64(11)
S(1)–C(13)	1.796(4)	C(1)–As(1)–Fe(2)	114.62(11)
		C(7)–As(1)–C(1)	100.1(2)
		C(13)–S(1)–Fe(2)	111.52(12)
		C(13)–S(1)–Fe(1)	111.64(13)

The <sup>1</sup>H-NMR spectrum of **1** at room temperature exhibits, in addition to the phenyl resonances of the SPh group, a sharp singlet at δ 1.90, integrating to three protons and a further singlet at δ 1.52 of the same intensity which may be assigned to the two methyl groups attached to arsenic. The fact that they are inequivalent on the NMR timescale at room temperature implies that the butterfly structure for the complex found in the crystal structure, in which the Fe–S–Fe and Fe–As–Fe wings are non-coplanar, is maintained in solution. The ‘wing-flapping’ fluxional process identified by Vahrenkamp [8] for the symmetrically bridged complex, [Fe<sub>2</sub>(CO)<sub>6</sub>(μ-AsMe<sub>2</sub>)<sub>2</sub>] at temperatures greater than 70°C, which renders the two methyl groups in this molecule equivalent, is not operative for **1** at room temperature.

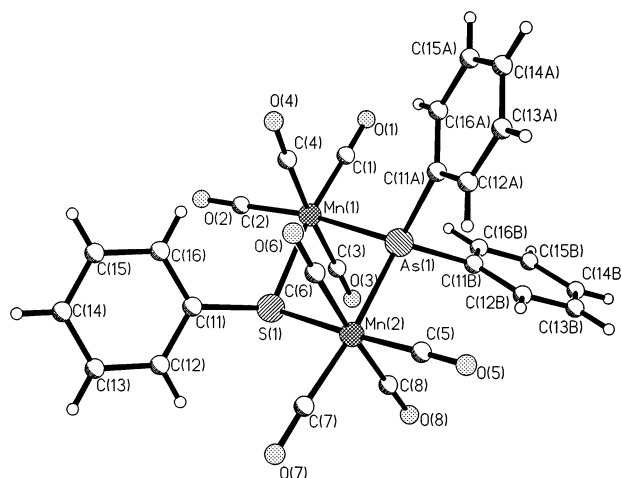


Fig. 3. Molecular structure of [Mn<sub>2</sub>(CO)<sub>8</sub>(μ-AsPh<sub>2</sub>)(μ-SPh)] (**3**) including atom numbering scheme.

The two different methyl groups are also apparent in the  $^{13}\text{C}$ -NMR spectrum at room temperature, in which signals at  $\delta$  11.0 and 4.0 are observed. Phenyl resonances due to the SPh group are also present, as is a single carbonyl resonance at  $\delta$  210.6. If an approximately octahedral environment is assumed for the iron atom, some fluxional process must occur to render the carbonyl groups equivalent. This may be a dissociative site-exchange process or a non-dissociative reorientation of the  $\text{Fe}(\text{CO})_3$  groups.

Table 3  
Selected bond lengths (Å) and angles ( $^\circ$ ) for  $\text{Mn}_2(\text{CO})_8(\mu\text{-AsPh}_2)(\mu\text{-SPh})$  (3)

Mn(1)–As(1)	2.4642(8)	S(1)–Mn(1)–As(1)	78.90(3)
Mn(2)–As(1)	2.4674(7)	S(1)–Mn(2)–As(1)	78.77(3)
Mn(1)–S(1)	2.4132(10)	Mn(2)–As(1)–Mn(1)	99.27(3)
Mn(2)–S(1)	2.4164(10)	Mn(2)–S(1)–Mn(1)	102.16(4)
As(1)–C	1.969(3), 1.970(3)	C(11A)–As(1)–Mn(1)	115.64(10)
S(1)–C(11)	1.791(3)	C(11A)–As(1)–Mn(2)	115.06(10)
Mn–C <sub>axial</sub>	1.854(4)–1.871(4)	C(11B)–As(1)–Mn(1)	116.40(9)
Mn–C <sub>equatorial</sub>	1.808(4)–1.843(4)	C(11B)–As(1)–Mn(2)	113.87(10)
		C(11A)–As(1)–C(11B)	97.62(13)
		C(11)–S(1)–Mn(1)	117.52(13)
		C(11)–S(1)–Mn(2)	111.09(11)

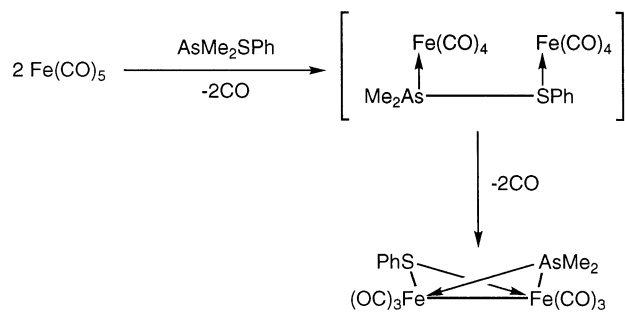


Fig. 4. Possible reaction mechanism for formation of complex 1.

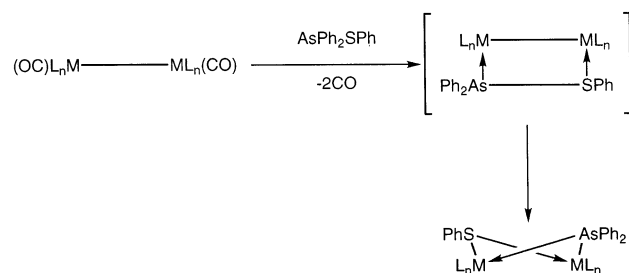


Fig. 5. Possible reaction mechanism for formation of complexes 2 [ $\text{ML}_n = \text{FeCp}(\text{CO})$ ] and 3 [ $\text{ML}_n = \text{Mn}(\text{CO})_4$ ].

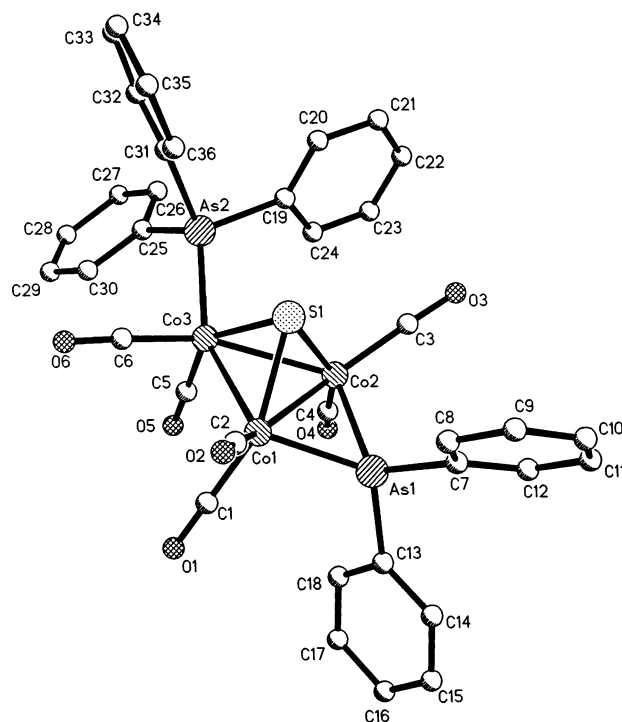


Fig. 6. Molecular structure of  $[\text{Co}_3(\mu_3\text{-S})(\mu\text{-AsPh}_2)(\text{CO})_6(\text{AsPh}_3)]$  (4) including atom numbering scheme. Hydrogen atoms have been omitted for clarity.

Table 4  
Selected bond lengths (Å) and angles ( $^\circ$ ) for  $\text{Co}_3(\mu_3\text{-S})(\mu\text{-AsPh}_2)(\text{CO})_6(\text{AsPh}_3)$  (4)

Co(1)–Co(2)	2.526(2)	Co(1)–Co(2)–Co(3)	59.41(5)
Co(1)–Co(3)	2.533(2)	Co(1)–Co(3)–Co(2)	59.13(5)
Co(2)–Co(3)	2.585(2)	Co(2)–Co(1)–Co(3)	61.47(5)
Co(1)–S(1)	2.182(3)	S(1)–Co(1)–Co(2)	54.47(8)
Co(2)–S(1)	2.176(3)	S(1)–Co(1)–Co(3)	53.91(8)
Co(3)–S(1)	2.160(3)	S(1)–Co(2)–Co(1)	54.69(8)
Co(1)–As(1)	2.296(2)	S(1)–Co(2)–Co(3)	53.11(8)
Co(2)–As(1)	2.310(2)	S(1)–Co(3)–Co(1)	54.71(8)
Co(3)–As(2)	2.333(2)	S(1)–Co(3)–Co(2)	53.68(8)
As–C <sub>phenyl</sub>	1.933(9)–1.957(9)	Co(2)–S(1)–Co(1)	70.84(9)
Co–C <sub>carbonyl</sub>	1.751(12)–1.784(12)	Co(3)–S(1)–Co(2)	73.20(9)
C–O <sub>carbonyl</sub>	1.129(12)–1.172(12)	Co(3)–S(1)–Co(1)	71.38(9)
		As(1)–Co(1)–Co(2)	57.01(5)
		As(1)–Co(2)–Co(1)	56.47(5)
		Co(1)–As(1)–Co(2)	66.52(6)
		S(1)–Co(1)–As(1)	93.52(9)
		S(1)–Co(2)–As(1)	93.29(9)
		S(1)–Co(3)–As(2)	99.98(9)

## 2.2. Reaction of $\text{AsPh}_2(\text{SPh})$ with $[\text{FeCp}(\text{CO})_2]_2$

Co-thermolysis of equimolar amounts of  $\text{AsPh}_2\text{SPh}$  and  $[\text{FeCp}(\text{CO})_2]_2$  in refluxing toluene for 4 h produced, in addition to two faint orange bands which were not collected, the green product,  $[\text{Fe}_2\text{Cp}_2(\text{CO})_2(\mu\text{-AsPh}_2)(\mu\text{-SPh})]$  (2) in 27% yield. Complex 2 has been characterised

by IR,  $^1\text{H}$ - and  $^{13}\text{C}$ -NMR spectroscopy, mass spectrometry and microanalysis. In addition, the complex has been the subject of a single crystal X-ray diffraction study.

The molecular structure of **2** is shown in Fig. 2. Selected bond lengths and angles are presented in Table 2. The complex crystallizes with one molecule of dichloromethane in the lattice per two molecules of **2**. This solvent molecule is disordered over two possible sites as displayed in the Figure.

The two iron atoms in **2** are bridged by a  $\text{AsPh}_2$  ligand and by a SPh ligand. In addition, each iron is ligated by one carbonyl group and a cyclopentadienyl ligand. Since the bridging ligands, the cyclopentadienyl rings and the carbonyl act as three-, five- and two-electron donors, respectively, each iron atom has 18 electrons and so a metal–metal bond would not be expected. The  $\text{Fe}\cdots\text{Fe}$  distance of 3.564 Å suggests that this is the case and that the two metal centres are held together by virtue of the bridging ligands only.

The central  $\text{Fe}_2\text{AsS}$  unit adopts a ‘butterfly’ structure with the As and S atoms in the wing-tip positions. However, the angle between the  $\text{Fe}-\text{As}-\text{Fe}$  and  $\text{Fe}-\text{S}-\text{Fe}$  planes at  $163.4^\circ$  means that there is a maximum deviation from planarity of only 0.13 Å. The arsenido and thiolato groups are displaced onto the same side of the molecule as the cyclopentadienyl rings and the

$\text{Fe}$ -carbonyl vectors are approximately perpendicular to the metal–metal axis.

### 2.3. Reaction of $\text{AsPh}_2(\text{SPh})$ with $[\text{Mn}_2(\text{CO})_{10}]$

Co-thermolysis of  $[\text{Mn}_2(\text{CO})_{10}]$  and one equivalent of  $\text{AsPh}_2(\text{SPh})$  in toluene, heated with stirring in an autoclave at  $140^\circ\text{C}$  for 12 h gave a small amount of unreacted  $[\text{Mn}_2(\text{CO})_{10}]$  and yellow  $[\text{Mn}_2(\text{CO})_8(\mu\text{-AsPh}_2)(\mu\text{-SPh})]$  (**3**) in 44% yield. Complex **3** has been characterised by IR,  $^1\text{H}$ - and  $^{13}\text{C}$ -NMR spectroscopy, mass spectrometry and microanalysis and by a single crystal X-ray diffraction study.

The molecular structure of **3** is shown in Fig. 3. Selected bond lengths and angles are presented in Table 3. The two manganese atoms in this complex are bridged by one  $\text{AsPh}_2$  group and one SPh ligand. In addition, each metal centre is ligated by four carbonyl groups, two located axially and two equatorially. This completes an approximately octahedral arrangement about each manganese atom. No metal–metal bond is predicted by application of the eighteen-electron rule and the long  $\text{Mn}\cdots\text{Mn}$  separation of 3.758 Å is inconsistent with a bonding interaction between the two metal centres.

While the  $\text{As}-\text{Mn}-\text{S}$  angles of  $78.90(3)$  and  $78.77(3)^\circ$  are marginally smaller than the  $\text{P}-\text{Mn}-\text{S}$  angles found

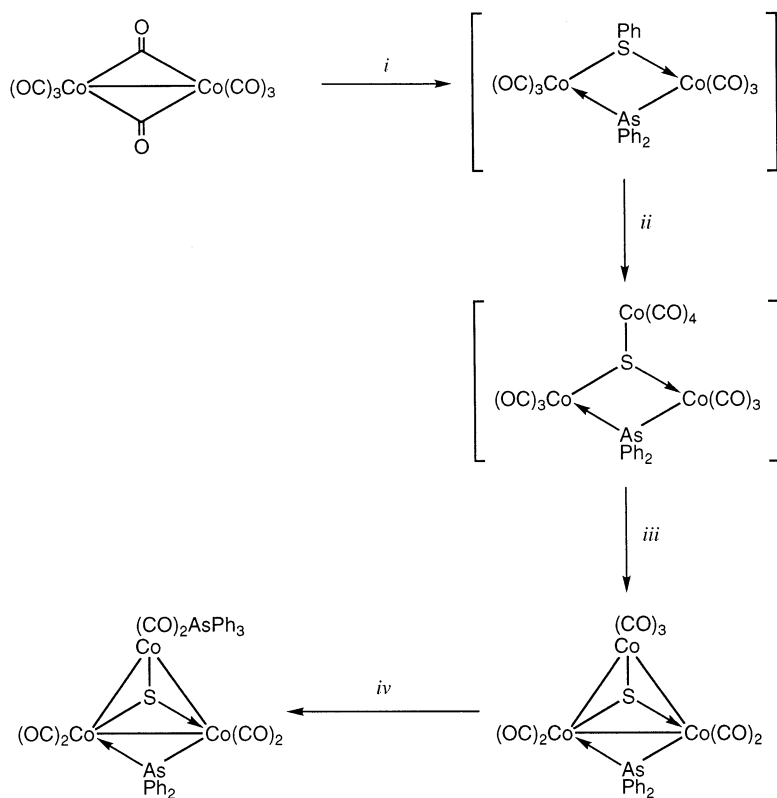


Fig. 7. Possible reaction mechanism for formation of complex **4**: (i) +  $\text{AsPh}_2(\text{SPh})$ ,  $-2\text{CO}$ ; (ii) +  $\text{Co}_2(\text{CO})_8$ ,  $-\text{PhCo}(\text{CO})_4$ ; (iii)  $-3\text{CO}$ ; (iv)  $\text{AsPh}_3$ .

Table 5  
X-ray crystallographic and data processing parameters for complexes **1**, **2**, **3** and **4**

Complex	<b>1</b>	<b>2</b>	<b>3</b>	<b>4</b>
Instrument	Rigaku Raxis-IIc	Rigaku AFC5R	Siemens P4	Rigaku AFC5R
$\lambda$ (Å)	0.71069	0.71069	0.71073	0.71069
Formula	C <sub>14</sub> H <sub>11</sub> AsFe <sub>2</sub> O <sub>6</sub> S	C <sub>30</sub> H <sub>25</sub> AsFe <sub>2</sub> O <sub>2</sub> S·0.5 CH <sub>2</sub> Cl <sub>2</sub>	C <sub>26</sub> H <sub>15</sub> AsMn <sub>2</sub> O <sub>8</sub> S	C <sub>36</sub> H <sub>25</sub> As <sub>2</sub> Co <sub>3</sub> O <sub>6</sub> S
<i>M</i>	493.91	678.64	762.24	912.25
Colour and habit of crystal	Orange prism	Dark green prism	Yellow prism	Red–brown prism
Crystal size (mm)	0.36 × 0.22 × 0.20	0.42 × 0.25 × 0.25	0.48 × 0.36 × 0.32	0.30 × 0.15 × 0.10
Crystal system	Monoclinic	Triclinic	Triclinic	Triclinic
Space group	<i>P</i> 2 <sub>1</sub> / <i>c</i>	$\bar{P}$ 1	$\bar{P}$ 1	$\bar{P}$ 1
Unit cell dimensions				
<i>a</i> (Å)	13.856(2)	10.214(2)	9.7748(18)	11.640(2)
<i>b</i> (Å)	22.189(2)	11.125(2)	11.460(2)	18.370(3)
<i>c</i> (Å)	18.261(3)	14.632(2)	13.6233(18)	9.426(2)
$\alpha$ (°)		96.840(10)	92.562(14)	101.13(2)
$\beta$ (°)	94.98(2)	100.360(10)	98.148(14)	110.03(2)
$\gamma$ (°)		116.340(10)	114.834(13)	72.710(10)
<i>V</i> (Å <sup>3</sup> )	5593.2(13)	1427.9(4)	1361.7(4)	1798.7(6)
<i>Z</i>	12	2	2	2
$\mu$ (Mo– <i>K</i> <sub>α</sub> ) (mm <sup>-1</sup> )	3.453	2.359	2.256	3.294
$\theta$ -range (°)	1.45–25.28	2.10–25.00	1.26–22.00	2.52–22.50
Limiting <i>hkl</i> indices	–16 ≤ <i>h</i> ≤ 16, –26 ≤ <i>k</i> ≤ 26, –21 ≤ <i>l</i> ≤ 21	–12 ≤ <i>h</i> ≤ 10, 0 ≤ <i>k</i> ≤ 13, –17 ≤ <i>l</i> ≤ 17	–1 ≤ <i>h</i> ≤ 18, –1 ≤ <i>k</i> ≤ 19, –20 ≤ <i>l</i> ≤ 19	0 ≤ <i>h</i> ≤ 12, –18 ≤ <i>k</i> ≤ 19, –10 ≤ <i>l</i> ≤ 9
Reflections collected	27335	5311	8960	4969
Independent reflections	9584	5030	7420	4692
Data/restraints/parameters	9584/0/649	5007/43/371	7420/102/541	4676/0/433
<i>S</i> on <i>F</i> <sup>2</sup>	1.489	1.071	0.980	1.046
Final <i>R</i> indices <sup>a</sup> [ <i>I</i> > 2σ( <i>I</i> )]	<i>R</i> <sub>1</sub> = 0.0831, <i>wR</i> <sub>2</sub> = 0.1484	<i>R</i> <sub>1</sub> = 0.0370, <i>wR</i> <sub>2</sub> = 0.0914	<i>R</i> <sub>1</sub> = 0.0341, <i>wR</i> <sub>2</sub> = 0.0879	<i>R</i> <sub>1</sub> = 0.0478, <i>wR</i> <sub>2</sub> = 0.0991
<i>R</i> indices (all data)	<i>R</i> <sub>1</sub> = 0.0942, <i>wR</i> <sub>2</sub> = 0.1586	<i>R</i> <sub>1</sub> = 0.0664, <i>wR</i> <sub>2</sub> = 0.1660	<i>R</i> <sub>1</sub> = 0.0472, <i>wR</i> <sub>2</sub> = 0.0934	<i>R</i> <sub>1</sub> = 0.1557, <i>wR</i> <sub>2</sub> = 0.2182
Weights <i>a</i> , <i>b</i> <sup>a</sup>	0.0324 and 16.5869	0.0474 and 0.6058	0.0574 and 0.1902	0.0334 and 0.5534
Largest difference peak and hole (eÅ <sup>-3</sup> )	0.394 and –0.487	0.468 and –0.661	0.534 and –0.419	0.525 and –0.513

<sup>a</sup>  $S = [\sum w(F_o^2 - F_c^2)^2 / (n - p)] / \Omega$  where *n* is number of reflections and *p* is the total number of parameters,  $R_1 = \sum ||F_o| - |F_c|| / \sum |F_o|$ ,  $wR_2 = \sum [w(F_o^2 - F_c^2)^2] / \sum [w(F_o^2)^2] \Omega$ ,  $w^{-1} = [\sigma^2(F_o)^2 + (aP)^2 + bP]$ ,  $P = [\max(F_o^2, 0) + 2(F_c^2)] / 3$ .

in the analogous ‘butterfly’ complex, [Mn<sub>2</sub>(CO)<sub>8</sub>(μ-PPh<sub>2</sub>)(μ-SPh)] [**3**] (79.0(1) and 79.0(1)°), the Mn–S–Mn angle is slightly larger for **3** than for the analogue (102.16(4)° **3** vs. 100.2(1)°).

There are slight changes in the other geometric parameters of the core which must be attributable to the substitution of phosphorus for arsenic. To accommodate the larger arsenic atom, the manganese atoms move further apart (Mn···Mn: 3.678 Å in [Mn<sub>2</sub>(CO)<sub>8</sub>(μ-PPh<sub>2</sub>)(μ-SPh)], 3.758 Å in **3**) but since the Mn–As bonds are significantly longer than the Mn–P bonds (2.4642(8) and 2.4674(7) Å vs. 2.401(2) and 2.393(2) Å) the Mn–As–Mn angle becomes 99.27(3)°, which is slightly smaller than the Mn–P–Mn angle in [Mn<sub>2</sub>(CO)<sub>8</sub>(μ-PPh<sub>2</sub>)(μ-SPh)] (100.4(1)°).

The Mn–C bonds to the carbonyls *cis* to the bridging groups are significantly longer than those to the *trans* carbonyls [M–C<sub>ax</sub>: 1.854(4)–1.871(4) Å; M–C<sub>eq</sub>: 1.808(4)–1.843(4) Å], an observation most reasonably

explained in terms of the *trans* influence of the bridging ligands.

The <sup>1</sup>H-NMR spectrum of **3**, as expected, contains resonances corresponding to phenyl protons only and phenyl carbon resonances are also observed in the <sup>13</sup>C spectrum. In the case of complex **3** there are clearly two sets of four-line signals, one with the *ipso*-carbon at δ 140.1 and the other with the *ipso*-carbon at δ 137.7. The ratio of intensities is approximately 1:2.

The first of these signals is assigned to the phenyl ring attached to sulfur and the second to the two rings bound to arsenic. Since the two rings attached to arsenic appear to be in the same chemical environment, the RS group must be fluxional. In addition, the Mn<sub>2</sub>AsS framework must be planar or if, in solution, the molecule retains the solid-state butterfly structure where the Mn–As–Mn and Mn–S–Mn ‘wings’ are non-coplanar, a fluxional, ‘wing-flapping’ process must be operative in solution, which would also render the two phenyl groups on arsenic equivalent.

Similar conclusions can be reached by an analysis of the carbonyl region of the  $^{13}\text{C}$ -NMR spectrum. A signal at  $\delta$  217.6 is assigned to the four carbonyls *cis* to the bridging ligands. Two further signals at  $\delta$  214.9 and 211.4 are of equal intensity and each of approximately half the intensity of the first signal. These two signals are ascribed to the four carbonyls *trans* to the bridging ligands. Two of these carbonyl groups project onto the same side of the molecule as the  $\text{AsPh}_2$  group while the other two carbonyls are directed towards the SPh moiety.

#### 2.4. Mechanism of bimetallic product formation

Reaction of the thioarsines,  $\text{AsR}_2(\text{SPh})$  [ $\text{R} = \text{Me}, \text{Ph}$ ] with the metal carbonyl complexes  $[\text{Fe}(\text{CO})_5]$ ,  $[\text{FeCp}(\text{CO})_2]$  and  $[\text{Mn}_2(\text{CO})_{10}]$  most likely proceeds via a dinuclear intermediate with a four-electron donor bridging  $\text{AsR}_2\text{-SR}$  ligand (Figs. 4 and 5), obtained by substitution of a carbonyl ligand from each metal centre. In the reaction of  $[\text{Co}_2(\mu\text{-RCCR})(\text{CO})_6]$  with  $\text{P}_2\text{Ph}_4$  similar dinuclear species have been isolated as stable products [12]. Subsequent cleavage of the As–S bond would generate one thiolato and one arsenido ligand. If these groups adopt bridging modes, they both act as three electron donors. The extra two electrons donated to the metals require rupture of the M–M bond in order to maintain adherence to the effective atomic number rule; thus complexes **2** and **3** are generated. In the case of complex **1**, however, there is no Fe–Fe bond to break. To maintain an electron count of eighteen at both iron centres, an Fe–Fe bond forms with concomitant loss of one carbonyl group from each metal atom.

#### 2.5. Reaction of $[\text{Co}_2(\text{CO})_8]$ with $\text{AsPh}_2(\text{SPh})$

Stirring  $[\text{Co}_2(\text{CO})_8]$  with one equivalent of  $\text{AsPh}_2(\text{SPh})$  in dichloromethane at room temperature for 20 h. gave red–brown  $[\text{Co}_3(\mu_3\text{-S})(\text{CO})_6(\mu\text{-AsPh}_2)(\text{AsPh}_3)]$  **4** in 49% yield. Complex **4** has been characterised by IR,  $^1\text{H}$ - and  $^{13}\text{C}$ -NMR spectroscopy, mass spectrometry and microanalysis and by a single crystal X-ray diffraction study.

The molecular structure of **4** is shown in Fig. 6. Selected bond lengths and angles are collected in Table 4. The molecule is constructed around a distorted tetrahedral core, containing three cobalt atoms and an apical sulfur. A diphenylarsenido group bridges Co(1) and Co(2), coordinating these atoms pseudo-equatorially. Each cobalt is further ligated by two carbonyl ligands, one located equatorially and the other at the axial site. The remaining equatorial position on Co(3) is occupied by a triphenylarsine molecule. The structure adopted resembles that of the phosphorus-containing analogue of complex **4**,  $[\text{Co}_3(\mu_3\text{-S})(\mu\text{-PPh}_2)(\text{CO})_6(\text{PPh}_3)]$  [3].

The Co(1)–Co(2) bond at 2.526(1) Å is the shortest of the three Co–Co bonds, presumably due to the constraints of the arsenido bridge, although it is longer than the corresponding bond in the phosphorus analogue (2.496(2) Å) since arsenic has a larger covalent radius. The triphenylarsine molecule is ligated equatorially, which places it on the same side of the complex as Co(2) and thus renders Co(1) and Co(2) inequivalent. This provides some explanation for the disparity in the lengths of the remaining metal–metal bonds [Co(1)–Co(3) 2.533(2) Å and Co(2)–Co(3) 2.585(2) Å] and also for the inequality of the Co–As(1) bond lengths (2.296(2) and 2.310(2) Å).

In the  $^{13}\text{C}$ -NMR spectrum of **4**, two equal intensity phenyl signals are observed with *ipso*-carbons located at  $\delta$  143.8 and 142.8. A more intense phenyl signal with an *ipso*-carbon resonance at  $\delta$  136.2 is assigned to the three equivalent phenyl rings of the  $\text{AsPh}_3$  ligand. The other two signals are due to the phenyl groups of the bridging  $\mu\text{-AsPh}_2$  unit. Since one ring projects onto the same side of the cluster as the apical sulfur, and the other is located on the opposite side of the molecule, the two rings occupy dissimilar environments which accounts for the two distinct groups of signals.

The reaction of  $\text{AsPh}_2(\text{SPh})$  with  $[\text{Co}_2(\text{CO})_8]$  parallels that of the thiophosphine,  $\text{PPh}_2(\text{SPh})$  with  $[\text{Co}_2(\text{CO})_8]$ . Given the temperature at which the reaction occurs and the ease with which  $[\text{Co}_2(\text{CO})_8]$  fragments to give  $\text{Co}(\text{CO})_4$ , it is reasonable to suggest a mechanism involving radicals. One possibility, shown in Fig. 7, is based on that proposed by Solan for the thiophosphine reaction [3]. The initial formation of a mixed-bridged dicobalt complex is reasonable, since analogous complexes can be synthesized from other dimeric metal carbonyls and  $\text{AsPh}_2(\text{SPh})$  (see **2** and **3**). This is followed by loss of the phenyl group from sulfur and concomitant S–Co bond formation. Cleavage of an S–C bond also takes place, for example, in the generation of the related species,  $[\text{Co}_3(\mu_3\text{-S})(\text{CO})_9]$  from  $[\text{Co}_2(\text{CO})_8]$  and  $\text{PhSH}$  [13]. Metal–metal bond formation could then occur with loss of carbon monoxide to give  $[\text{Co}_3(\mu_3\text{-S})(\mu\text{-AsPh}_2)(\text{CO})_7]$ . The phosphido analogue of this complex was isolated in the reaction of  $\text{PPh}_2(\text{SPh})$  and  $[\text{Co}_2(\text{CO})_8]$  but with  $\text{AsPh}_2(\text{SPh})$ , the reaction proceeds further to give the  $\text{AsPh}_3$  derivative only.

### 3. Conclusions

On reaction with the metal carbonyl complex  $[\text{Fe}(\text{CO})_5]$ , the As–S bond of the thioarsine  $\text{AsMe}_2(\text{SPh})$  is readily cleaved with both fragments of the cleaved ligand being retained as bridging groups within the di-iron product. The same process occurs when the thioarsine  $\text{AsPh}_2(\text{SPh})$  reacts with

[FeCp(CO)<sub>2</sub>]<sub>2</sub>, [Mn<sub>2</sub>(CO)<sub>10</sub>] or [Co<sub>2</sub>(CO)<sub>8</sub>], although in the last case, S–C bond cleavage also occurs and a trimetallic product result. From these studies it appears that the reactivity of the thioarsines parallels that of the more extensively studied thiophosphine analogues.

#### 4. Experimental

All reactions were carried out under an atmosphere of dry, oxygen-free nitrogen, using solvents which were freshly distilled from the appropriate drying agent.

Infrared spectra were recorded in *n*-hexane or CH<sub>2</sub>Cl<sub>2</sub> solution in 0.5 mm NaCl cells, using a Perkin–Elmer Paragon 1000 Fourier-Transform spectrometer or a Perkin–Elmer 1600 series spectrometer. Fast atom bombardment mass spectra were obtained on a Kratos MS890 instrument. Fast ion bombardment mass spectra were obtained on a Kratos MS50 instrument. Nitrobenzyl alcohol was used as a matrix.

<sup>1</sup>H- and <sup>13</sup>C-NMR spectra were recorded on Bruker AM400 or WM250 spectrometers using the solvent resonance as an internal standard. Microanalyses were performed by the Microanalytical Department of the University of Cambridge.

Preparative thin-layer chromatography was carried out on 1 mm plates prepared at the University Chemical Laboratory, Cambridge. Column chromatography was performed on Kieselgel 60 (70–230 mesh). The products are given in order of decreasing *R<sub>f</sub>* values. All reagents were obtained from commercial suppliers and used without further purification.

The reaction of AsR<sub>2</sub>Cl with NaSPh was employed to prepare AsR<sub>2</sub>(SPh) (R = Me, Ph). The procedure was based on the literature preparation of AsPh<sub>2</sub>[S(C<sub>5</sub>H<sub>11</sub>)] [14] but the sodium mercaptide was generated using sodium hydride rather than sodium metal. AsMe<sub>2</sub>Cl [15,16] was prepared by reduction of cacodylic acid. The oxide, (AsPh<sub>2</sub>)<sub>2</sub>O [17,18], was synthesised by reaction of PhMgBr and As<sub>2</sub>O<sub>3</sub>. Treatment of this oxide with HCl generated AsPh<sub>2</sub>Cl [18,19].

##### 4.1. Reaction of AsMe<sub>2</sub>SPh with [Fe(CO)<sub>5</sub>]

AsMe<sub>2</sub>SPh (263 mg, 1.23 mmol) and [Fe(CO)<sub>5</sub>] (241 mg, 1.23 mmol) were refluxed in 50 ml toluene. After removal of reaction solvents under vacuum, the residue was dissolved in a minimum quantity of CH<sub>2</sub>Cl<sub>2</sub> and adsorbed onto silica. The silica was pumped dry and transferred to the top of a silica chromatography column. Elution with 19:1 hexane–acetone gave orange crystalline [Fe<sub>2</sub>(CO)<sub>6</sub>(μ-AsMe<sub>2</sub>)<sub>2</sub>] (84 mg, 28%) and yellow crystalline [Fe<sub>2</sub>(CO)<sub>6</sub>(μ-

AsMe<sub>2</sub>)(SPh)] (**1**) (109 mg, 36%). Crystals of **1** suitable for X-ray diffraction were grown by slow evaporation of an *n*-hexane solution of the complex at –18°C. Complex **1** (found: C, 34.05%; H, 2.20%. C<sub>14</sub>H<sub>11</sub>AsFe<sub>2</sub>O<sub>6</sub>S. Requires: C, 34.05%; H, 2.24%). Mass spectrum *m/e* 494 (*M*<sup>+</sup>): *M*<sup>+</sup> – *n*(CO) (*n* = 1–6). IR (*v*<sub>max</sub> cm<sup>–1</sup> hexane): 2061m, 2039w, 2023vs, 1993s, 1978s. <sup>1</sup>H-NMR (CDCl<sub>3</sub>): δ 7.4–7.1 (m, 5H, *Ph*), δ 1.90 (s, 3H, *Me*), δ 1.52 (s, 3H, *Me*). <sup>13</sup>C-NMR: δ 210.6 (CO), δ 139.9–127.5 (*Ph*), δ 11.0 (s, *Me*), δ 4.0 (s, *Me*).

##### 4.2. Reaction of AsPh<sub>2</sub>(SPh) with [FeCp(CO)<sub>2</sub>]<sub>2</sub>

AsPh<sub>2</sub>(SPh) (477 mg, 1.41 mmol) and [FeCp(CO)<sub>2</sub>]<sub>2</sub> (500 mg, 1.41 mmol) were refluxed in 50 ml toluene for 4 h. After removal of the reaction solvent, the residue was redissolved in the minimum amount of dichloromethane and applied to the base of silica TLC plates. Elution with hexane/ethyl acetate (9:1) gave two faint orange bands which were not collected and green–brown crystalline [Fe<sub>2</sub>Cp<sub>2</sub>(CO)<sub>2</sub>(μ-AsPh<sub>2</sub>)(μ-SPh)] (**2**) (240 mg, 27%). Crystals suitable for diffraction were grown by slow evaporation from a solution of CH<sub>2</sub>Cl<sub>2</sub>/*n*-hexane at 0°C. Complex **2** (Found: C, 56.32%; H, 3.83%. C<sub>30</sub>H<sub>25</sub>AsFe<sub>2</sub>O<sub>2</sub>S. Requires: C, 56.64%; H, 3.96%). Mass spectrum *m/e* 636 (*M*<sup>+</sup>): *M*<sup>+</sup> – *n*(CO) (*n* = 1–2). IR (*v*<sub>max</sub> cm<sup>–1</sup> CH<sub>2</sub>Cl<sub>2</sub>): 1954s. <sup>1</sup>H-NMR (CDCl<sub>3</sub>): δ 7.7–7.0 (m, 15H, *Ph*), δ 4.34 (s, 10H, *Cp*). <sup>13</sup>C-NMR: δ 223.6 (s, CO), δ 140.0–124.5 (*Ph*), δ 78.8 (s, *Cp*).

##### 4.3. Reaction of AsPh<sub>2</sub>(SPh) with [Mn<sub>2</sub>(CO)<sub>10</sub>]

AsPh<sub>2</sub>(SPh) (426 mg, 1.26 mmol) and [Mn<sub>2</sub>(CO)<sub>10</sub>] (500 mg, 1.26 mmol) were dissolved in 50 ml toluene and heated with stirring in an autoclave at 140°C for 12 h. After removal of reaction solvents under vacuum, the residue was dissolved in a minimum quantity of dichloromethane and adsorbed onto silica. The silica was pumped dry and transferred to the top of a silica chromatography column. Elution with 6:4 hexane–CH<sub>2</sub>Cl<sub>2</sub> gave a small amount of unreacted [Mn<sub>2</sub>(CO)<sub>10</sub>] and yellow [Mn<sub>2</sub>(CO)<sub>8</sub>(μ-AsPh<sub>2</sub>)(μ-SPh)] (**3**) (373 mg, 44%). Crystals of **3** suitable for X-ray diffraction were grown by slow evaporation at 0°C of an *n*-hexane–CH<sub>2</sub>Cl<sub>2</sub> solution of the complex. Complex **3** (Found: C, 46.34%; H, 2.19%. C<sub>26</sub>H<sub>15</sub>AsMn<sub>2</sub>O<sub>8</sub>S. Requires: C, 46.45%; H, 2.25%). Mass spectrum *m/e* 672 (*M*<sup>+</sup>): *M*<sup>+</sup> – *n*(CO) (*n* = 1–4,8). IR (*v*<sub>max</sub> cm<sup>–1</sup> CH<sub>2</sub>Cl<sub>2</sub>): 2063m, 2006s, 1958m. <sup>1</sup>H-NMR (CDCl<sub>3</sub>): δ 7.7–7.2 (m, 15H, *Ph*). <sup>13</sup>C-NMR: δ 217.6 (s, 4CO), δ 214.9 (s, 2CO), δ 211.4 (s, 2CO), δ 140.1–126.8 (*Ph*).

#### 4.4. Reaction of $\text{AsPh}_2(\text{SPh})$ with $[\text{Co}_2(\text{CO})_8]$

$[\text{Co}_2(\text{CO})_8]$  (500 mg, 1.46 mmol) and  $\text{AsPh}_2(\text{SPh})$  (493 mg, 1.46 mmol) were dissolved in 100 ml dichloromethane and stirred for 20 h. After removal of reaction solvents under vacuum, the residue was dissolved in a minimum quantity of  $\text{CH}_2\text{Cl}_2$  and adsorbed onto silica. The silica was pumped dry and transferred to the top of a silica chromatography column. Elution with 7:3 hexane– $\text{CH}_2\text{Cl}_2$  gave green  $[\text{Co}_3(\mu_3\text{-S})(\text{CO})_6(\mu\text{-AsPh}_2)(\text{AsPh}_3)]$  (**4**) (435 mg, 49%). Crystals suitable for X-ray diffraction were grown by slow evaporation at 0°C of a  $\text{CH}_2\text{Cl}_2$ –*n*-hexane solution of **4**. Complex **4** (Found: C, 47.06%; H, 2.63%.  $\text{C}_{36}\text{H}_{25}\text{As}_2\text{Co}_3\text{O}_6\text{S}$ . Requires: C, 47.40%; H, 2.76%). Mass spectrum  $m/e$  912 ( $M^+$ );  $M^+ - n(\text{CO})$  ( $n = 1-6$ ). IR ( $\nu_{\text{max}}$   $\text{cm}^{-1}$  hexane): 2046m, 2025w, 2014vs, 1997s.  $^1\text{H-NMR}$  ( $\text{CDCl}_3$ ):  $\delta$  7.7–7.2 (m, 25H, *Ph*).  $^{13}\text{C-NMR}$ :  $\delta$  143.8–128.6 (*Ph*).

#### 4.5. X-ray crystal structure determinations

Details of data collection, refinement and crystal data are listed in Table 5. Lorentz-polarisation corrections were applied to the data of all the compounds.

The positions of the metal atoms and most of the non-hydrogen atoms were located from direct methods [20], and the remaining non-hydrogen atoms were revealed from subsequent difference-Fourier syntheses. Refinement was based on  $F^2$ . All hydrogen atoms were placed in calculated positions with displacement parameters equal 1.2 and 1.5  $U_{\text{eq}}$  of the parent carbon atoms for phenyl and methyl hydrogen atoms, respectively. Semi-empirical absorption corrections using  $\psi$ -scans were applied to the data of **2**, **3** and **4**. All non-hydrogen atoms were assigned anisotropic displacement parameters in the final cycles of full-matrix least-squares refinement.

### 5. Supplementary material

Crystallographic data for the structural analyses have been deposited with the Cambridge Crystallographic Data Centre, CCDC Nos. 116576–116579 for compounds **1–4**, respectively. Copies of this information may be obtained free of charge from The Director, CCDC, 12 Union Road, Cambridge CB2 1EZ (Fax: +44-1223-336-033; e-mail deposit@ccdc.cam.ac.uk or www: http://www.ccdc.cam.ac.uk).

### Acknowledgements

We thank the Defence Research Agency (Fort Halstead) for financial support to J.D.K and the EPSRC and the Cambridge Crystallographic Data Centre for support to J.E.D.

### References

- [1] B.E. Job, R.A.N. McLean, D.T. Thompson, *J. Chem. Soc. Chem. Commun.* (1966) 895.
- [2] G. Le Borgne, R. Mathieu, *J. Organomet. Chem.* 208 (1981) 201.
- [3] A.J. Edwards, A. Martín, M.J. Mays, D. Nazar, P.R. Raithby, G.A. Solan, *J. Chem. Soc. Dalton Trans.* (1993) 355.
- [4] G.E. Pateman, Ph.D. Thesis, University of Cambridge, 1996.
- [5] (a) A.J. Edwards, A. Martín, M.J. Mays, P.R. Raithby, G.A. Solan, *J. Chem. Soc. Chem. Commun.* (1992) 1416. (b) G. Conole, M. Kessler, M.J. Mays, G.E. Pateman, G.A. Solan, *Polyhedron* 17 (1998) 2993.
- [6] (a) R.M. Bozorth, *J. Am. Chem. Soc.* 45 (1923) 1621; (b) J. Kopf, K. von Deuten, G. Klar, *Inorg. Chim. Acta* 37 (1980) 67. (c) B.J. McKerley, K. Reinhardt, J.L. Mills, G.M. Reisner, J.D. Kopf, I. Bernal, *Inorg. Chem. Acta* 31 (1978) L411. (d) I. Bernal, H. Brunner, W. Meier, H. Pfisterer, J. Wachter, M.L. Ziegler, *Angew. Chem. Int. Ed. Engl.* 23 (1984) 438. (e) H. Brunner, H. Kauermann, B. Nuber, J. Wachter, M.L. Ziegler, *Angew. Chem. Int. Ed. Engl.* 25 (1986) 557. (f) H. Brunner, B. Nuber, L. Poll, J. Wachter, *Angew. Chem. Int. Ed. Engl.* 32 (1993) 1627. (g) H. Brunner, L. Poll, J. Wachter, *J. Organomet. Chem.* 471 (1994) 117. (h) H. Brunner, L. Poll, J. Wachter, *Polyhedron* 15 (1996) 573. (i) H. Brunner, H. Kauermann, L. Poll, B. Nuber, J. Wachter, *Chem. Ber.* 129 (1996) 657.
- [7] J. Chatt, D.A. Thornton, *J. Chem. Soc.* (1964) 1005.
- [8] (a) E. Keller, H. Vahrenkamp, *Chem. Ber.* 110 (1977) 430. (b) H. Vahrenkamp, E. Keller, *Chem. Ber.* 112 (1979) 1991.
- [9] C.H. Wei, L.F. Dahl, *Inorg. Chem.* 2 (1963) 328.
- [10] L.-C. Song, R.-J. Wang, Y. Li, H.-G. Wang, J.-T. Wang, *Acta. Chim. Sin.* 48 (1990) 867.
- [11] L.-C. Song, Q.-M. Hu, *J. Organomet. Chem.* 414 (1991) 219.
- [12] A.J.M. Caffyn, M.J. Mays, G.A. Solan, D. Braga, P. Sabatino, G. Conole, M. McPartlin, H.R. Powell, *J. Chem. Soc. Dalton Trans.* (1991) 3103.
- [13] D.L. Stevenson, V.R. Magnuson, L.F. Dahl, *J. Am. Chem. Soc.* 89 (1967) 3727.
- [14] W. Steinkopf, I. Schubert, S. Schmidt, *Chem. Ber.* 61 (1928) 678.
- [15] V. Auger, *Compt. Rendu* 142 (1906) 1151.
- [16] W. Steinkopf, W. Mieg, *Chem. Ber.* 53 (1920) 1013.
- [17] F. Sachs, H. Kantoriwicz, *Chem. Ber.* 41 (1908) 2767.
- [18] F.F. Blicke, F.D. Smith, *J. Am. Chem. Soc.* 51 (1929) 1558.
- [19] A.E. Goddard, in: J. Newton Friend (Ed.), *Textbook of Inorganic Chemistry (Part II)*, vol. XI, Charles Griffin, London, 1930, p. 113.
- [20] SHELXL (PC version 5.03) Siemens Analytical Instruments, Madison, WI, 1994.